

Interactions Between Charged Spheres in Divalent Counterion Solution

Niels Grønbech-Jensen and Keith M. Beardmore

Theoretical Division, Los Alamos National Laboratory, Los Alamos, New Mexico 87545

Philip Pincus

Department of Physics, University of California, Santa Barbara, California 93106

(August 5, 2018)

Abstract

We simulate model systems of charged spherical particles in their counterion solution and measure the thermodynamic pressure and the pair distribution function from which we derive effective potentials of mean force. For a system with only electrostatic and hard core interactions, we investigate the effective potential between two like-charged spheres in divalent counterion solution as a function of concentration. We find a strong attractive interaction for high concentration and a global repulsive effective interaction for dilute systems. The results indicate a first order phase transition in sphere-counterion density as a function of global concentration and the effective sphere-sphere potentials in the dilute (solvated) regime suggest significant density fluctuations due to short range local minima in the effective energy surface. Our results arise from a minimal approach model of several recent experiments on polystyrene latex particles in monovalent counterion solution.

The effective interactions between charged macromolecules in countercharged aqueous media have been assumed to be governed mainly by simple screened Coulomb behavior leading to overall repulsion between like charged objects [1–4]. This notion arises primarily from mean-field analyses, such as Poisson-Boltzmann equations, of the statistical counterion distribution, and leads to the well known Derjaguin-Landau-Verwey-Overbeek (DLVO) purely repulsive effective potential between charged colloidal spherical macroions [3,4]. However, recent experiments have indicated that the effective interaction can indeed be attractive in dense suspensions of, e.g., polystyrene latex particles in aqueous solutions with monovalent counterions [5–15]. These experiments, performed with very low salt concentrations, have observed inhomogeneous colloid densities under certain conditions and almost perfectly homogeneous densities under others. Some of the experiments observe the attractive potentials only when the colloidal spheres are suspended between glass walls [6,7] and it is consequently a speculation whether the effective attraction is mediated by these walls or if the walls merely provide a confinement of phase space such that the attraction is enhanced. Recent advances for investigating the effective interactions have been made [16] by performing direct numerical simulations of charged colloidal spheres and their monovalent counterions in confined space and only repulsive interactions were found.

As the present state of theoretical predictions is almost entirely limited to the trivial repulsive behavior between fractionally screened like-charged objects, we have carried out simulations of a simple system which exhibits strong effective short as well as long range attractions between like-charged spherical objects in their neutralizing counterion solution. This is intended as helping to construct a successful theoretical approach describing the complex phase behavior of charged colloidal suspensions. The purpose of this paper is therefore not to give a direct interpretation of the recent experiments on polystyrene latex particles, but instead point to a simple system exhibiting a phenomenon that a theoretical approach should reproduce.

We present simulations of charged colloidal spheres and their counterions confined in a cubic box volume $V \equiv L^3$, where L is the box length in each direction, with periodic boundary conditions applied such that a finite bulk concentration is simulated. Finite concentration is important since Coulomb interactions between spherical objects ($\sim 1/r$) are inferior to entropic repulsion ($\sim \ln r$) at large distances. The equilibrium distance between any charged spherical objects at finite temperature is consequently divergent in the limit of $N/V \rightarrow 0$, where N is the number of spherical objects; thus, the effective interaction is always repulsive in the dilute limit. We will focus on a system with divalent counterions in order to clearly demonstrate the importance of concentration and correlation effects, which are absent in mean field treatments leading to, e.g., the DLVO potential. We demonstrate that the effective potential between two spheres, as derived from the pair distribution function, can become attractive in finite concentration. Our simulations are performed as a minimal approach in that only long-range Coulomb interactions and short-range volume exclusions contribute to the evolution of the system.

The model under consideration is given by the Overdamped Langevin equation of motion for the i th particle:

$$\nu_i \dot{\bar{r}}_i = -\nabla_i E + \bar{n}_i(t) , \quad (1)$$

where \bar{r}_i is the normalized coordinate of the i th particle moving with a normalized friction

coefficient ν_i (note that neither the friction coefficient nor the time normalization has any importance for the equilibrium properties of the system). The total normalized energy E of the system is given by,

$$E = \sum_{i=1}^N \sum_{j>i}^N \left(\frac{q_i q_j}{\varepsilon} V(r_{ij}) + W_{hc}(r) \right), \quad (2)$$

where

$$W_{hc}(r) = \begin{cases} \frac{A_{ij}}{(r_{ij}-r_{ij}^0)^{12}} - \frac{B_{ij}}{(r_{ij}-r_{ij}^0)^6}, & (r_{ij}-r_{ij}^0)^6 < 2A_{ij}/B_{ij} \\ 0, & (r_{ij}-r_{ij}^0)^6 \geq 2A_{ij}/B_{ij} \end{cases}. \quad (3)$$

A_{ij} and B_{ij} are the Lennard-Jones volume exclusion parameters. Notice that we only consider the short range *repulsive* part of the Lennard-Jones potential. N is the total number of coordinates (spheres and counterions) and eq_i is the charge of the i th particle. The normalized Coulomb interaction between charges eq_i and eq_j at a normalized distance r_{ij} is represented by $\frac{q_i q_j}{\varepsilon} V(r_{ij})$, with dielectric constant ε (for details on exact summation of Coulomb interactions in orthorhombic systems, see Ref. [17]). The thermal equilibrium with the surroundings, i.e., with the water which is not considered except as a homogeneous dielectric, is maintained by the noise term $\bar{n}_i(t)$ which is linked to the dissipation-fluctuation theorem [18] by the uncorrelated white Gaussian distribution,

$$\langle \bar{n}_i(t) \rangle = \bar{0}, \quad \langle \bar{n}_i(t) \cdot \bar{n}_j(t') \rangle = 6\nu_i \frac{k_B T}{E_0} \delta_{ij} \delta(t-t'), \quad (4)$$

where δ_{ij} is the Kronecker delta function and $\delta(t-t')$ the Dirac delta function. Boltzmann's constant is denoted k_B , the temperature is T , and the energy is normalized to $E_0=1$ kcal/mol. The factor, 6, is due to \bar{n} being a three dimensional vector. Throughout this paper we have chosen divalent counterions, sphere charges of $q_{sp} = -10$, $A_{ij} \approx 21 \cdot 10^3$, $B_{ij} \approx 30$, and $\varepsilon = 80$ in order to mimic bulk screening of water. The hard core parameter, r_{ij}^0 , is chosen as $r_{ij}^0 = 0$ for counterion counterion interactions, $r_{ij}^0 = 5.5$ for counterion sphere interactions, and $r_{ij}^0 = 11$ for sphere sphere interactions. Each simulation is initiated with random, non-overlapping positions of the counterions and spheres and a large number of time steps, of order 10^8 , are discarded before accumulating the pair distribution density function, $\rho(r)$, between spheres. In equilibrium, this density is directly related to the Boltzmann factor,

$$\rho(r) \sim \exp(-W(r)/k_B T), \quad (5)$$

where $W(r)$ is the effective potential of mean force (PMF). Inverting this relationship and normalizing the potential to the value at maximum distance $r = L/2$, we obtain the derived effective PMF from,

$$W(r) = -k_B T \ln \left(\frac{\rho(r)}{\rho(L/2)} \right). \quad (6)$$

Figure 1 displays the PMF between two spheres and their accompanying divalent counterions in a simulation box of volume $V = L^3$. The friction coefficients are set to $\nu_{ci} = 1$ for

counterions and $\nu_{sp} = 15$ for spheres with the accompanying reduced time step $dt = 0.005$. The resulting sphere-sphere PMF, derived over $\sim 10^8$ time steps, reveals strongly attractive behavior for small L (lower curves), but as L is increased, the available volume increases, and the minimum characteristic for attraction lifts above zero (normalized to the potential at distance $L/2$) and eventually disappears. The minimum of the PMF, W_{min} , is shown in Fig. 2 as a function of the simulated volume. Here we observe how the minimum (relative to the value at $L/2$) of the effective potential depends on the volume. At a volume $\approx (120\text{\AA})^3 \approx 2 \cdot 10^3 \text{nm}^3$ the potential at $L/2$ becomes the global minimum, which clearly indicates a transition from close packed spheres being preferred in small volumes to separated spheres being statistically preferred at larger volumes.

However, as is obvious from Fig. 1, the spheres can be attracted to each other at short distances even if the global PMF minimum is at $L/2$. This feature arises from the much stronger interaction that exists between a counterion and two closely spaced spheres when compared to the interaction between a counterion and a single sphere. This then leads to a compact state of the two spheres with their counterions spatially correlated around them. The barrier height (PMF) in energy going from the compact state to the maximum separation ($L/2$) is shown in Fig. 3, where we find a significant barrier, i.e., a local minimum for the compact state, well into the volume regime where the global minimum of the PMF is at maximum separation.

The PMF potentials shown in figure 1 are in strong contrast to the DLVO potential, which is given by [3,4]

$$W_{DLVO}(r) = \frac{k_B T}{E_0} q_{sp}^2 \left(\frac{e^{\kappa a}}{1 + \kappa a} \right)^2 e^{-\kappa r} \frac{\lambda_B}{r} + W_{hc}(r), \quad (7)$$

where a is the radius of the spheres and the hard core interaction between two spheres is given by W_{hc} . The two characteristic length scales, λ_B and κ , are given by,

$$\lambda_B = \frac{e^2}{4\pi\epsilon_0\epsilon k_B T}, \quad (8)$$

$$\kappa^2 = 4\pi\lambda_B \frac{M}{V} q_{ci}^2, \quad (9)$$

where M is the number of counterions and q_{ci} is the counterion valency. The DLVO potential is obviously repulsive and monotonically decaying with distance.

Studying the PMF gives information about the spatial correlations within the sample simulation, but it does not reveal the overall nature of global attraction versus repulsion of an ensemble. In order to study if the system tends to collapse or expand, we have calculated the thermodynamic pressure,

$$\begin{aligned} p_T &= - \left(\frac{\partial \mathcal{F}}{\partial V} \right)_{T,N} \\ &= N \frac{k_B T}{V} + \frac{1}{3V} \left\langle \sum_{i=1}^N \sum_{j>i}^N \bar{r}_{ij} \cdot \bar{f}_{ij} \right\rangle + \frac{\langle U_{el} \rangle}{3V}, \end{aligned} \quad (10)$$

where \mathcal{F} is Helmholtz's free energy and $\langle \dots \rangle$ denotes a temporal average. The first term on the right hand side is the *thermal* contribution to the pressure, the second is the contribution

from the virial of all *hard core* interactions (4), and the last is the *electrostatic* contribution, U_{el} being the total electrostatic energy of the system.

Figure 4a shows the total pressure, p_T , versus the volume for one simulated sphere and its counterions in a cubic box. In agreement with the PMFs visualized in figure 1, we find an effective attraction (negative pressure) for high concentration of spheres and a repulsive effective interaction (positive pressure) for dilute systems. This behavior of pressure as a function of concentration indicates a first order phase transition from a solvated state of spheres at low concentration to a collapsed state of spheres at high concentration. However, the global pressure cannot reveal the short range local minima in the PMFs observed in figure 1. These local minima, which persist far into the dilute limit, will result in local density fluctuations of the solvated spheres. Note that the negative pressure is solely due to the electrostatic interactions since both the kinetic and the hard core contributions to the total pressure are always positive (see figure 4b, where the three individual pressure contributions are shown). The total pressure will, in the dilute limit, be entirely dictated by the thermal contribution (ideal gas) since the finite temperature will separate all spherical particles and thereby make the hard core and the electrostatic contributions negligible.

Also the pressure is in contrast to the DLVO analysis. Since the DLVO potential is purely repulsive, one can only expect positive pressures from such a treatment. The reason for the possibility of negative pressures in the “all particle” model lies in the overall charge neutrality of the system. It is clear that a charge neutral system composed of oppositely charged components is self-contracting at low temperatures (e.g., the sodium-chloride crystal) due to strong spatial correlations between the charged objects. However, the DLVO analysis only accounts for the counterion charge if it contributes to the screening of a sphere, and thus, the DLVO treatment does not maintain the overall charge neutrality of the system.

We have simulated a system of charged spheres in divalent counterion solution and demonstrated a very strong attractive effective potential between the like-charged spheres. The origin of the attraction lies in the strong correlation effects between counterions when the spheres are in a compact conformation. This simple result is in contrast to the effective (and always repulsive) DLVO potential, which is developed without considering the counterions as particles. However, our results are in agreement with other recent simulations of like-charged rods in divalent counterion solution [19] and theoretical considerations regarding like-charged plates [20]. Our simple simulations demonstrate that a successful theory explaining the complicated phase diagram of complex charged fluids needs to account for the correlated behavior of counterions, the global charge neutrality leading to the tensile pressure in figure 4, and the relationship between the sphere radius and the simulated volume responsible for the statistical distribution of counterions.

It is important to emphasize that our simulations are not meant to characterize real experiments quantitatively. The minimal approach model presented in this paper cannot account for any atomic or molecular detail that may be important for experiments. For example, including the effects of the solvent (water) as friction, noise, and bulk screening is a dramatic simplification of the true discrete nature of water molecules, which exhibit their discrete nature within the hydration shell. Also, neglecting the complexity of the dielectric mixture of water and spheres prevents our model from correctly simulating the electrostatic problem. Our simulations therefore address the validity of present theories, such as DLVO, which attempt to describe the minimal approach model described in this paper.

This work was performed under the auspices of the U.S. Department of Energy, supported in part by National Science Foundation grant DMR-9708646 and in part by funds provided by the University of California for the conduct of discretionary research by Los Alamos National Laboratory.

REFERENCES

- [1] J. Israelachvili, *Intermolecular and Surface Forces* (Academic Press, London, 1992).
- [2] H. M. Lindsey and P. M. Chaikin, *J. Chem. Phys.* **76**, 3774 (1982).
- [3] B. V. Derjaguin and L. Landau, *Physichochim. URSS* **14**, 633 (1941).
- [4] E. J. Verwey and J. T. G. Overbeek, *Theory of the Stability of Lyophobic Colloids* (Elsevier, Amsterdam, 1948).
- [5] B. V. R. Tata, M. Rajalakshmi, and A. K. Arora, *Phys. Rev. Lett.* **69**, 3778 (1992); T. Palberg and M. Würth, *Phys. Rev. Lett.* **72**, 786 (1994); B. V. R. Tata and A. K. Arora, *Phys. Rev. Lett.* **72**, 787 (1994).
- [6] J. C. Crocker and D. G. Grier, *Phys. Rev. Lett.* **77**, 1897 (1996).
- [7] A. E. Larsen and D. G. Grier, *NATURE* **385**, 230 (1997).
- [8] A. Sharma, S. N. Tan, and J. Y. Walz, *J. Colloid Interface Sci.* **190**, 392 (1997).
- [9] J. G. Daly and R. Hastings, *J. Phys. Chem.* **85**, 294 (1981).
- [10] A. K. Arora and R. Kesavamoorthy, *Solid State Commun.* **54**, 1047 (1985).
- [11] N. Ise, T. Okubo, M. Sugimura, K. Ito, and H. J. Nolte, *J. Chem. Phys.* **78**, 536 (1983).
- [12] N. Ise, H. Matsuoka, and K. Ito, *Macromolecules* **22**, 1 (1980).
- [13] R. Kesavamoorthy, M. Rajalakshmi, and C. B. Rao, *J. Phys. Condens. Matter* **1**, 7149 (1989).
- [14] N. Ise, H. Matsuoka, and H. Yoshida, *Faraday Discuss. Chem. Soc.* **90**, 153 (1990).
- [15] S. Yoshino, in *Ordering and Organization in Ionic Solutions*, eds. N. Ise and I. Sogami (World Scientific, Singapore, 1988), p. 449.
- [16] M. J. Stevens, M. L. Falk, and M. O. Robbins, *J. Chem. Phys.* **104**, 5209 (1996).
- [17] N. Grønbech-Jensen, *Int. J. Mod. Phys. C* **8**, 1287 (1997).
- [18] see, e.g., G. Parisi, *Statistical Field Theory* (Addison-Wesley, Redwood City, 1988) p. 326.
- [19] N. Grønbech-Jensen, R. J. Mashl, R. F. Bruinsma, and W. M. Gelbart, *Phys. Rev. Lett.* **78**, 2477 (1997).
- [20] I. Rouzina and V. A. Bloomfield, *J. Phys. Chem.* **100**, 9977 (1996).

FIGURES

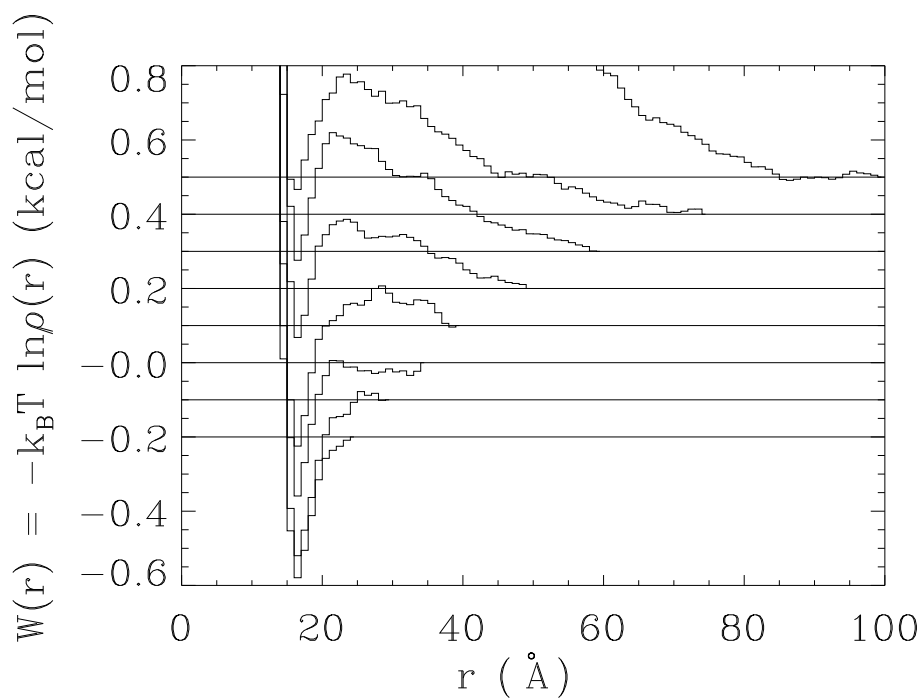


FIG. 1. Potentials of Mean Force for different simulated volumes. The potentials are set to zero at maximum separation, $L/2$, and the different potentials are off-set vertically in order to better distinguish the cases. Potentials of Mean Force are shown for (from the top): $L = 200\text{\AA}$, $L = 150\text{\AA}$, $L = 120\text{\AA}$, $L = 100\text{\AA}$, $L = 80\text{\AA}$, $L = 70\text{\AA}$, $L = 60\text{\AA}$, and $L = 50\text{\AA}$.

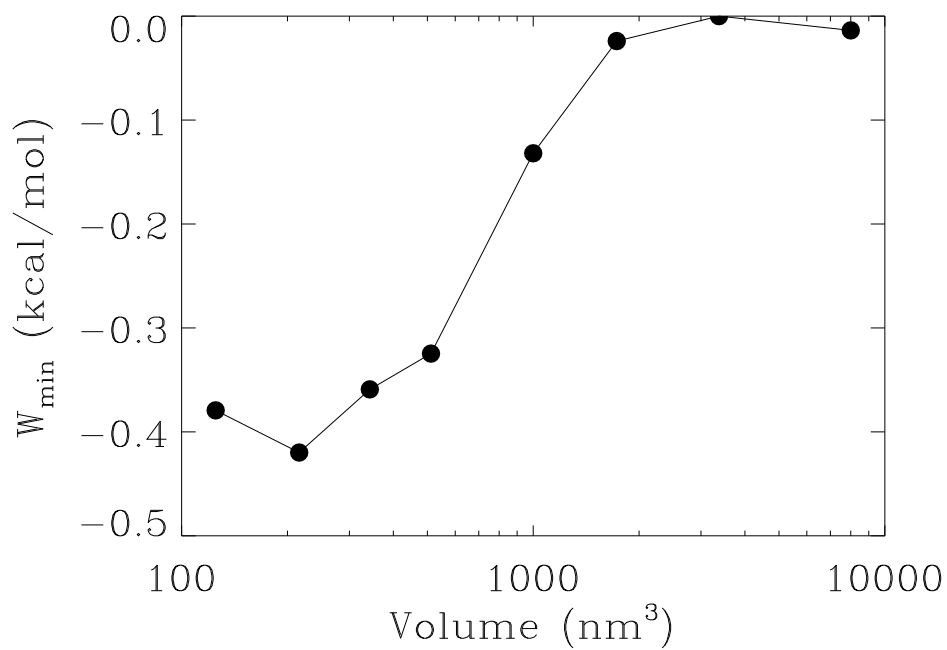


FIG. 2. Minimum of the potentials of mean force shown in Fig. 1 versus the simulated volume, $V = L^3$.

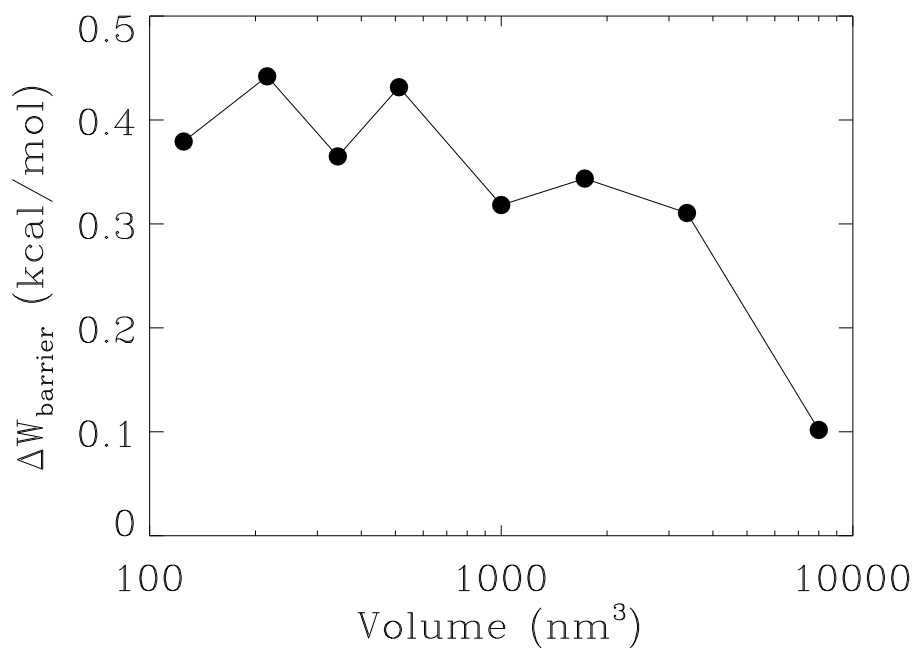


FIG. 3. Energy barrier height from the compact state ($r \approx 16$ in figure 1) to the local PMF maximum ($r \approx 22$ in figure 1) as a function of the simulated volume.

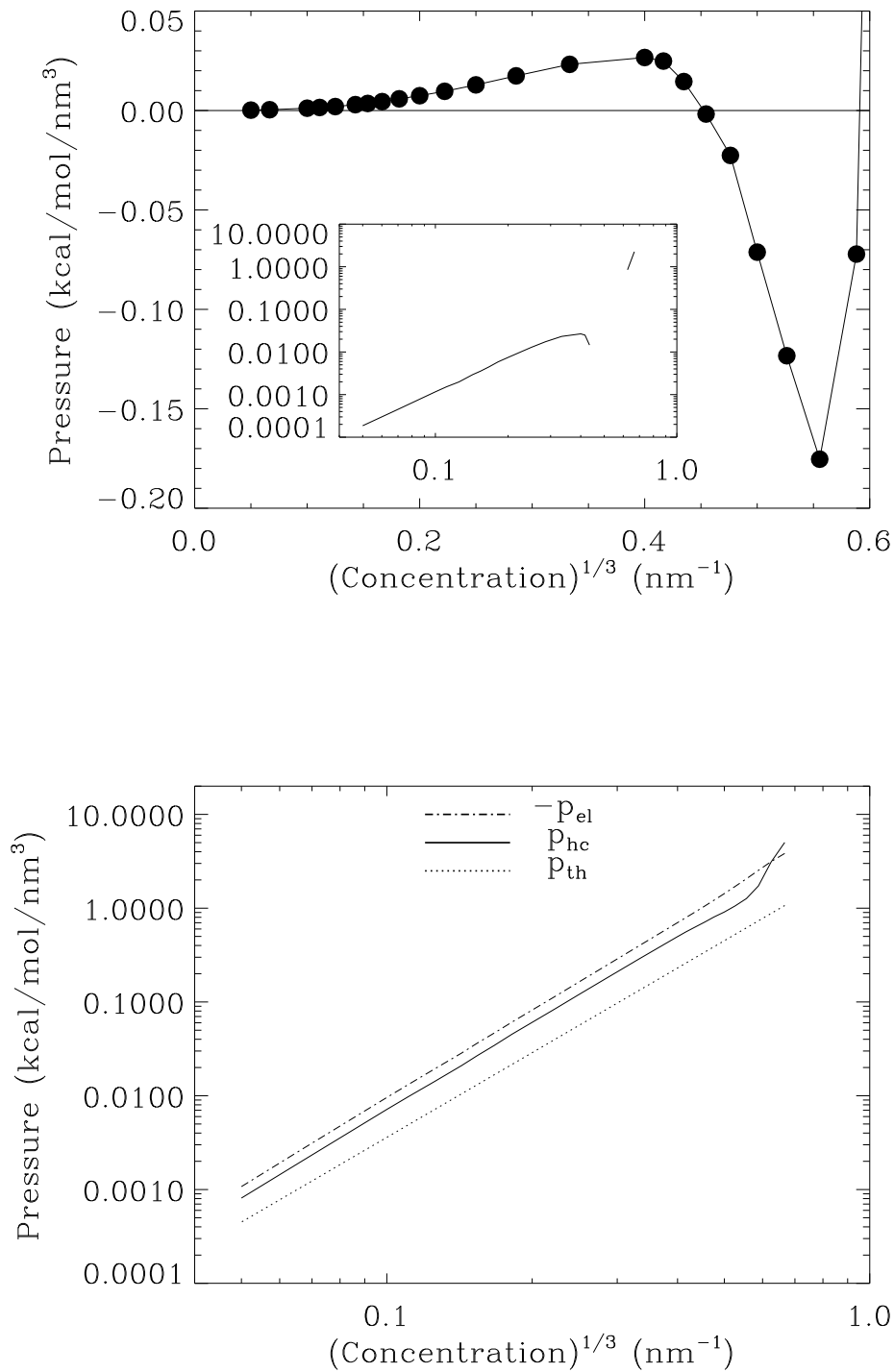


FIG. 4. (a) Magnitude of thermodynamic pressure of a system of one sphere and its counterions in a cubic box versus simulated volume. The inset shows the same data in a log-log representation. (b) Magnitude of the three contributions to the pressure shown in (a); thermal (dotted); hard core (solid); and the negative electrostatic (dash-dot).